

RESEARCH

Open Access



Study on Crack Resistance and Calculation Model of RAC Beams Strengthened with Prestressed CFRP

Yanting Ji¹, Sheng Sun^{2,3}, Aijiu Chen^{2*}, Fen Yang^{2,4}, Shihua Bai⁵ and Xiaoyan Han²

Abstract

With the development of recycled aggregate concrete (RAC), the recovery rate of construction waste is improved, and the pollution problem is alleviated. In particular, RAC beams strengthened with prestressed carbon fiber reinforced plastics (CFRP) can exhibit improved mechanical properties, expanding RAC application. Four groups of reinforced RAC beam specimens contained 0%, 40%, 70%, and 100% recycled coarse aggregate, respectively. Each group of beams was first pre-cracked and then strengthened by prestressed CFRP with one layer and two layers respectively. Finally, the bearing capacity tests were performed for these beams. The test results show that as the recycled coarse aggregate content increases, the cracking moment and ultimate load capacity of the beam decrease, while its crack width increases. As the CFRP layer increases, the deformation and crack width of the beam decreases, while the number of cracks increases. The prestressed CFRP also exhibited tensile and peeling failure. A beam deflection calculation model was established by introducing a coefficient k representing the interaction between recycled aggregate and CFRP. The influence coefficient of concrete elongation on the crack width and average crack spacing of the beam was modified, and the crack width analysis model of the beam was established. The calculated results are in good agreement with the experimental observations. It can provide reference for the application and design of recycled concrete beams strengthened with prestressed CFRP.

Keywords Prestressed CFRP, RAC, Beam, Strengthening, Crack resistance

1 Introduction

The rapid social and financial improvement has brought about a significant expansion of concrete construction, which has led to the overexploitation of existing

resources and damage to the ecological balance. Lots of construction and demolition waste simultaneously piles up, occupying land resources and causing environmental pollution (Xie et al., 2018; Yehia et al., 2015). For example, the UK generates around 110 million tonnes of construction waste each year (Medina et al., 2014); in the USA, its annual production is about 200–300 million tonnes (Lotfy et al., 2015). To address such problems, crushing waste concrete for reuse as a construction material has been proposed. This can conserve existing resources, reduce the accumulation of construction waste, relieve pressure on environmental pollution mitigation, and protect the ecological environment (Toledo et al., 2013; Wang et al., 2021).

However, due to the weak areas at the bonding interface between the recycled coarse aggregate and cement

Journal information: ISSN 1976-0485 / eISSN 2234-1315.

*Correspondence:

Aijiu Chen
caj@ncwu.edu.cn

¹ School of Water Conservancy, North China University of Water Resources and Electric Power, Zhengzhou 450046, China

² School of Civil Engineering and Communication, North China University of Water Resources and Electric Power, Zhengzhou 450045, China

³ China Railway NO.3 Engineering Group Co. Ltd, Jinzhong 030604, China

⁴ Zhengzhou Zoo, Zhengzhou 450008, China

⁵ Henan Zhongyu Engineering Consulting Group Co., Ltd., Zhengzhou 450000, China

Table 1 The physical properties of each aggregate

Aggregate type	Size (mm)	Fineness	Apparent density (kg/m ³)	Pile-up density (kg/m ³)	Mud content (%)	Water absorption (%)	Crushed index (%)
Recycled coarse	5–20	/	2490	1240	0.68	4.2	14.2
Coarse	5–20	/	2810	1360	0.47	1.0	9.0
Fine	0–4.75	2.9	2590	1420	1.8	1.3	/

mortar, the mechanical properties of RAC components are greatly reduced (Chen, 2013; Dimitriou et al., 2018; McNeil & Kang, 2013; Ozbakkaloglu et al., 2018). This can seriously affect the promotion and application for RAC. Therefore, active measures should be taken to strengthen RAC components, improve structural safety and thus expand the application of RAC. Many structural strengthening methods have been developed, such as the external prestress method (Zhao et al., 2019), the outsourcing steel method (Shakirov & Sulejmanov, 2021), and the steel plate bonding method (GB/T 50367-2013, 2013). However, these methods exhibit many defects. For instance, the reinforcement procedure is accompanied by intricate steps, and the steel elements, once exposed to the external environment, are prone to corrosion, leading to a reduction in the overall service life. Furthermore, considering the relatively higher density of steel compared to concrete, the incorporation of steel reinforcement results in an increase in the structural weight. These inherent drawbacks pose limitations on the widespread adoption and application of the aforementioned strengthening methods.

Carbon fiber reinforced plastics (CFRP) are extensively used for structural reinforcement due to their high strength, small thickness, high corrosion resistance, and high durability (Bakar et al., 2022; ElSafty et al., 2014; Huang et al., 2020; Kadhim et al., 2021). As the increase of CFRP layers, the compressive strength of concrete increases. The strengthening effects of CFRP on concrete with lower strength are more significant. It has been shown that the initial cracking load, ultimate bearing capacity, fatigue limit and shear strength of concrete beams strengthened by CFRP can increase by about 40%, 67%, 33%, and 25%–114%, respectively (Colalillo & Sheikh, 2012; Eljufout et al., 2021; Helal et al., 2020). Therefore, considering the advantages and good strengthening effect of CFRP, it can be a preferred technology for strengthening concrete structures.

In addition, it has been reported that prestressed CFRP can fully exhibit its structural performance and enhance strengthening effects (Gao et al., 2016; Huang et al., 2017; Song & Hou, 2017; Xue et al., 2010) showed an increase in flexural bearing capacity of 35.6% and 27.5–57.4% for beams strengthened with CFRP and prestressed CFRP

respectively. Thus, prestressed CFRP can facilitate the effective use of CFRP strength. In terms of the reliability of prestressed CFRP-reinforced concrete beams, (Liu et al., 2015) established a flexural bearing capacity model, Which provided a basis for analyzing and evaluating the reliability and safety of concrete structures strengthened by prestressed CFRP.

Although prestressed CFRP is effective and safe for strengthening concrete structures, it has been rarely used in RAC structures (Khan et al., 2021; Zhang et al., 2019), and existing research focuses more on materials (Chen et al., 2016). Therefore, in this paper, RAC beams with different recycled coarse aggregate contents were designed and strengthened with prestressed CFRP. The effects of recycled aggregate content and the number of prestressed CFRP layers on the deflection and crack width of RAC beams were explored. Based on the modified equivalent area of the steel bars and the ultimate compressive strain of concrete, a deflection calculation

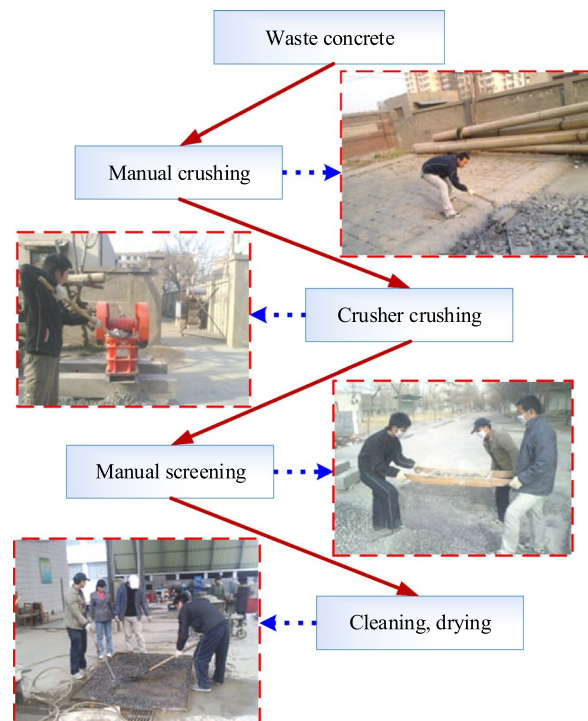


Fig. 1 Production process of recycled coarse aggregate

Table 2 Physical and mechanical properties of Ordinary Portland cement

Setting time (min)		Compressive strength (MPa)		Flexural strength (MPa)		Fineness (%)	Loss on ignition (%)
Initial	Final	3 days	28 days	3 days	28 days	3	2.3
180	280	29.5	46.8	5.4	8.0		

model of RAC beams strengthened by prestressed CFRP was proposed. The influence coefficient of concrete elongation on crack width and average crack spacing of the beams was revised, and the crack width analysis model of RAC beams strengthened by prestressed CFRP was established. It can provide a basis for engineering design and application of RAC.

2 Materials and Methods

2.1 Materials

Table 1 shows the physical properties of each aggregate used in the test. Fine aggregate is natural river sand. Recycled coarse aggregate was produced from concrete waste and belonged to Category II according to the Standard (GB/T 25177-2010, 2010). Fig. 1. shows its production process. The cementitious material is Ordinary Portland cement with a strength grade of 42.5 MPa. Table 2 shows its physical and mechanical properties. UT70-30 CFRP and adhesive resin were obtained from Japan Toray Company, in which the thickness of CFRP is 0.167 mm. Their mechanical properties are illustrated in Table 3.

2.2 Specimen Preparation

Four groups of reinforced RAC beams were prepared and each group included two RAC beams. The design strength of RAC was C35. The water-cement and sand

ratios were 0.5 and 35%, respectively. The recycled coarse aggregate content was selected as 0%, 40%, 70%, and 100%, respectively. The mixing ratio of RAC was designed according to Standard (JGJ 55-2011, 2011) (Table 4). Meanwhile, 6 concrete cubes of 100 mm³ and 6 concrete prisms of 150×150×300 mm³ were prepared and cured under the same conditions as RAC beams for 28 days. According to the specification (GB/T50081-2019, 2019), the compressive strength and splitting tensile strength of the concrete cube, the axial compressive strength and elastic modulus of the concrete prism were tested, and the mechanical properties of RAC are displayed in Table 5.

These RAC beams were 3000 mm long and had a cross-section of 150×300 mm². The concrete cover had a thickness of 25 mm. As shown in Fig. 2, two 14 mm diameter HRB400 bars were used as longitudinal stress steel bars, the stirrups along the beam shear span were arranged as Φ6@80, and two 10 mm diameter HPB235 bars were used as auxiliary steel bars, and the mechanical properties of steel bar as displayed in Table 6.

2.3 Test Program

The CFRP, which is bonded along the entire width of the beam's bottom surface, was strengthened using a tension tool (Chen et al., 2013), resulted in achieving a significantly

Table 3 Mechanical properties of CFRP and adhesive resin

Tensile strength (MPa)	Tensile elastic modulus (GPa)	Bending strength (MPa)	Elongation (%)	Interlaminar shear strength (MPa)	Adhesive tensile shear strength (MPa)
4059	242	822	1.71	49.6	9.08

Table 4 Mixing ratio of RAC beams (kg/m³)

Serial number	Cement	Water	Natural coarse aggregate	Natural fine aggregate	Recycled coarse aggregate	Additional water
RAC0	360	180	1209	651	0	0
RAC40	360	180	725	651	429	18.02
RAC70	360	180	363	651	750	31.50
RAC100	360	180	0	651	1071	44.98

Table 5 Mechanical properties of RAC (MPa)

Serial number	Compressive strength	Splitting tensile strength	Axial compressive strength f_c	Elastic modulus E_c
RAC0	57.0	3.84	49.7	31,920
RAC40	54.4	3.54	45.6	29,930
RAC70	50.8	3.18	44.0	29,840
RAC100	44.0	3.13	38.7	28,250

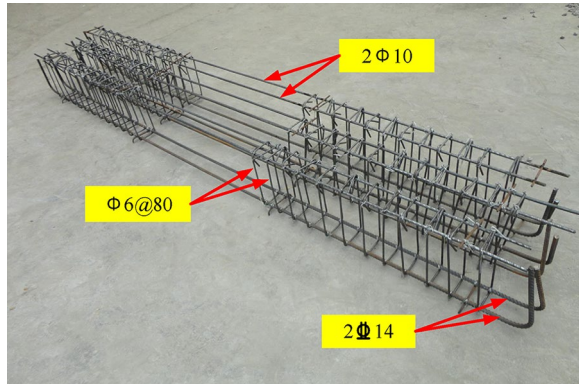


Fig. 2 Reinforcement arrangement for RAC beams

Table 6 Mechanical properties of steel bar

Serial number	Yield strength (MPa)	Ultimate strength (MPa)	Elastic modulus (GPa)
HRB400	370.6	480.8	198
HPB235	256.7	390.8	210
HPB235	242.5	356.3	206

high effective strain of up to 4000 $\mu\epsilon$. Three 100 mm wide CFRP strips were pasted on each beam side for U-hoop anchorage. The strain gauges for RAC and CFRP were BX120-100AA and BX120-5AA, respectively. Five strain

gauges were arranged at the heights of 32, 82, 132, 232, and 282 mm respectively on the mid-span side of the beam from bottom to top to verify the plane section assumption. Measure the mid-span deflection of the beam with a dial gauge. The strain data were collected using a YJSA static resistance strain instrument. Fig. 3. shows the CFRP paste, dial indicator, and strain gauge arrangement on the beam.

The load was applied to the beam under static loading. The load magnitude in each loading stage was controlled by a YJSA static resistance strain gauge connected to a transducer. The crack development in the beam was observed with a magnifying glass, and its crack width was measured with a microscope at 40x. To match the actual service condition of the structures, the RAC beams were pre-cracked according to the pre-cracking bending moments in Table 7 until the maximum crack width on the beams reached 0.20 mm. Upon completion of pre-cracking, the RAC beams underwent a strengthening process involving the application of one or two layers of CFRP. The notation RAC0I and RAC0II indicates that the recycled aggregate content in the beams is 0, and the CFRP reinforcement layers are denoted as I and II, respectively. To effectively test the working performance of the loading and information acquisition system, the reinforced beam was preloaded to 15 kN before the target loading and then loaded at a step of 10 kN. After the beam yielded, the loading was controlled by the mid-span displacement. A displacement of 3 mm was set as the loading level. The beam was gradually loaded until the beam failed.

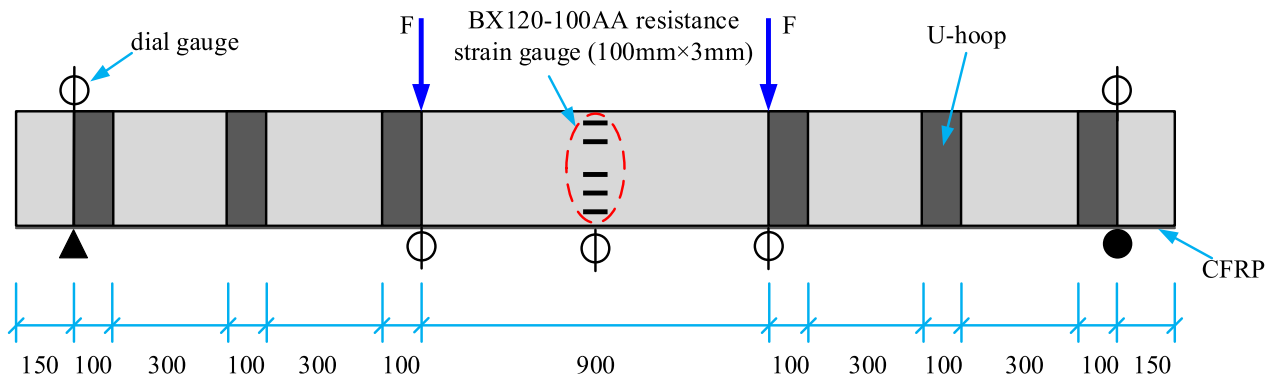


Fig. 3 RAC beam strengthened by prestressed CFRP (Unit: mm)

Table 7 Pre-cracking bending moment of reinforced RAC beams

Pre-cracking bending moment	RAC0	RAC40	RAC70	RAC100
M_p (kN-m)	32	32	31	30

3 Results

3.1 Failure Modes of RAC Beams

For the RAC beams strengthened by one layer of pre-stressed CFRP, small CFRP strips near the lateral edge of the beam first fractured before the load approached the ultimate value. Then, as the load increased, the CFRP suddenly broke, producing a loud cracking sound. The failure mode was therefore referred to as CFRP tensile failure, as illustrated in Fig. 4.

For the RAC beams strengthened by two layers of pre-stressed CFRP, the beams were partially crushed when the applied load approached the yield load, accompanied by a slight brittle sound during the loading. When approaching the ultimate load, the CFRP and concrete protection layer began to peel away from the main crack. Peel damage progressed towards the beam ends, and the peeling rate decreased near the U-hoop. As the increasing load, the CFRP at the U-hoop peeled off together with the protective concrete layer. Finally, the reinforced RAC beams were damaged. The beam failure is displayed in Fig. 5.

From Fig. 6, the stress process in beams has three stages, i.e., OA, AB, and BC. Stage OA was approximately regarded as the stage before beam cracking, i.e., the elastic stage. Stage AB was the crack development stage. In Stage BC, the beam was damaged. The concrete and steel



Fig. 4 Failure mode of RAC beams strengthened by one layer CFRP

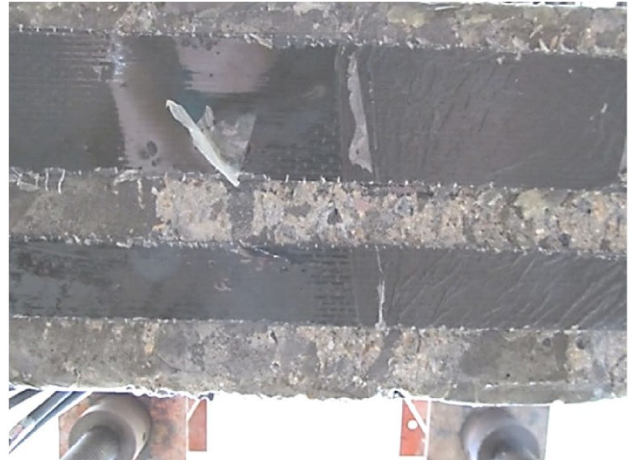


Fig. 5 Failure mode of RAC beams strengthened by two layers CFRP



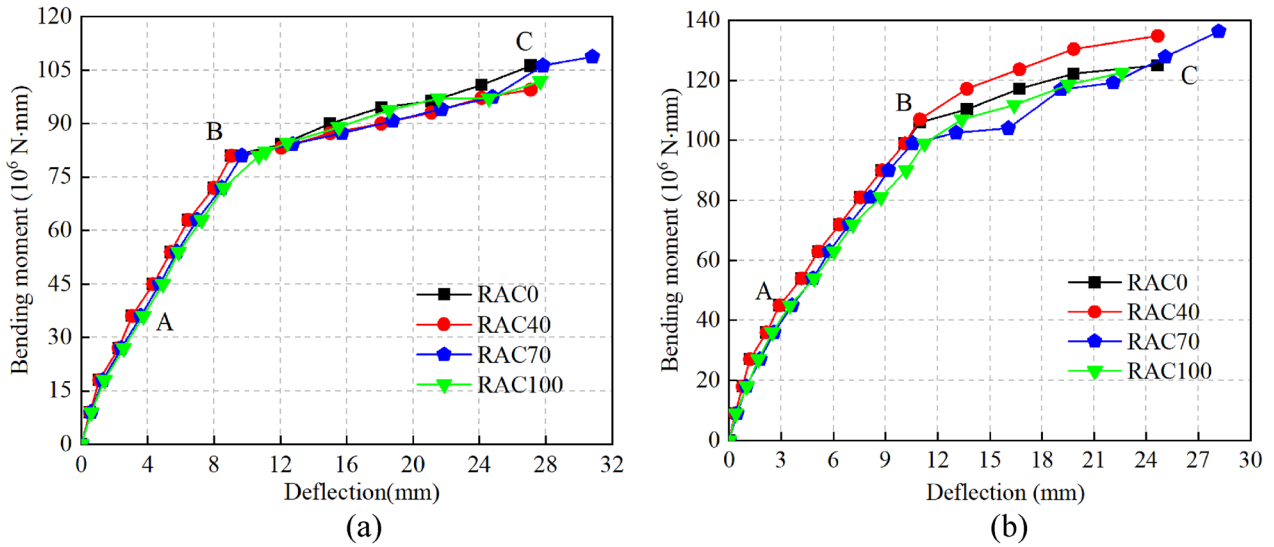


Fig. 6 Bending moment-deflection of RAC beams strengthened by different layers CFRP: **a** one layer; **b** two layers

bars reached their limit states, with significant cracks in the beam. The beam stiffness in these three stages (i.e., OA, AB, and BC) was expressed as B_{O-A} , B_{A-B} , and B_{B-C} , respectively. It is found that the average strains of the beams along the mid-span height showed an approximately linear relationship with the load from loading initiation to near-failure states. Thus, the beam strains along the height direction generally conform to the plane section assumption.

Fig. 6 shows that the bending moments of reinforced RAC beams strengthened by one layer and two layers of prestressed CFRP at yield were about 80 and 110 kN m, respectively. This indicates that CFRP further improved the beam stiffness. Furthermore, many microcracks derived from recycled coarse aggregate reduced the mechanical properties of beams. Therefore, strengthening beams with CFRP can restrain the beam displacement to a certain extent, and the suppression of beam deflection tends to decrease. This indicates that incorporating recycled aggregates reduced the beams' elastic modulus and deformation capacity and increased deflection.

3.2 Calculation of Beam Deflection

3.2.1 Elastic Stage

Two RAC beams with 40% recycled aggregate were taken as examples for analysis. The measured and Standard (GB 50010-2010, 2010) stiffness for the RAC beams strengthened by CFRP was significantly different (Fig. 7). Therefore, the stiffness calculation formula from the Standard was not suitable for this study.

Thus, based on the Standard (GB 50010-2010, 2010) and the crack development stage in reinforced RAC beams, a new stiffness calculation method was proposed for

prestressed concrete flexural members in the stage without cracks:

$$B_{OA} = 0.85kE_cI_0 \tag{1}$$

$$k = (0.9463 - 0.1046\rho)e^{0.0102A_{cf}} \tag{2}$$

$$I_0 = \frac{1}{12}bh^3 + bh\left(\frac{h}{2} - x_0\right)^2 + \alpha_s A_s (h_0 - x_0)^2 + \alpha'_s A'_s (x_0 - \alpha_{s1})^2 + \alpha_{cf} A_{cf} (h - x_0)^2 \tag{3}$$

$$\frac{1}{2}bx_0 + \alpha'_s A'_s (x_0 - \alpha'_s) = \frac{1}{2}b(h - x_0)^2 + \alpha_s A_s (h_0 - x_0) + \alpha_{cf} A_{cf} (h - x_0) \tag{4}$$

where k is a coefficient introduced to incorporate the role of recycled aggregate and CFRP; E_c represents the elastic modulus for RAC; I_0 represents the inertial moment of the converted section; ρ represents the recycled aggregate content; A_{cf} represents the actual bonding area for CFRP; A'_s is the area of compression reinforcement; α_{s1} indicates the distance from the resultant point of the compressed reinforcement to the compressed edge of the section; $\alpha_{s1}' = E_{s1}'/E_c$, $\alpha_s = E_s/E_c$ and $\alpha_{cf} = E_{cf}/E_c$; E_{s1}' and E_{cf} represent the elastic modulus of compressed steel bars and CFRP, respectively. The meanings of other parameters are shown in the Standard (GB 50010-2010, 2010). x_0 represents the height of the compression zone of the concrete, which can be determined by using the principle that the compression and tension zones of the

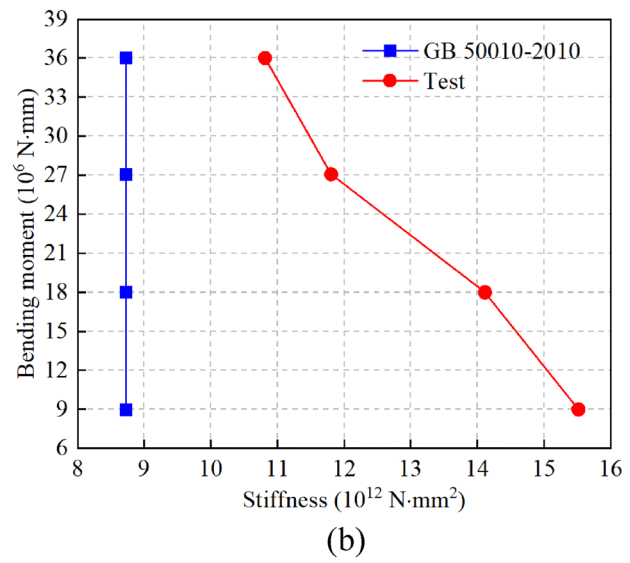
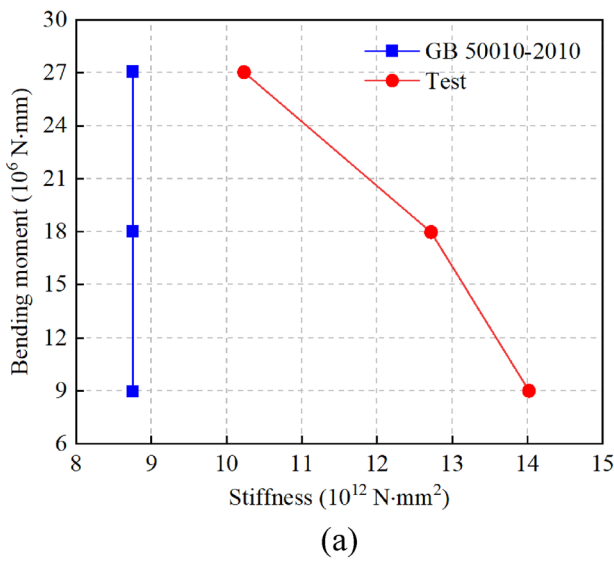


Fig. 7 Stiffness of RAC beams: **a** RAC40I; **b** RAC40II

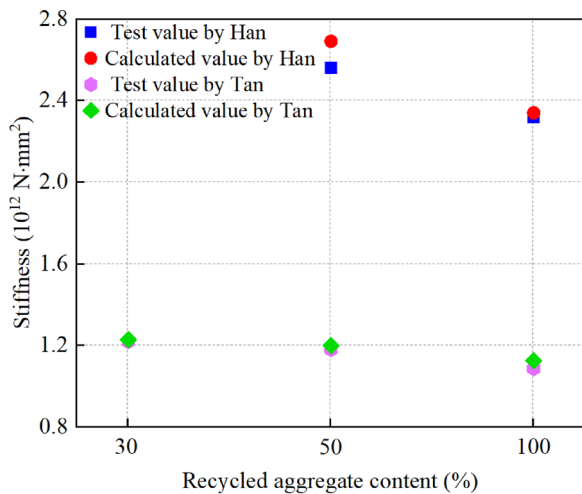


Fig. 8 Comparison between calculated and measured stiffness of RAC beams

concrete are equal to the bending section and axial area moment of the beam.

The coefficient k introduced in this paper was verified using the data from two references (Han et al., 2019) and (Tan et al., 2019). The calculation results were consistent with the measurement (Fig. 8). This indicates that it was reasonable to consider the coefficient k at the recycled aggregate content ρ .

To further verify the rationality of coefficient k , the data from references (Xie et al., 2019) and (Zhao et al., 2017) were used. The calculated and measured stiffness values were compared and analyzed (Fig. 9). The calculated and

measured stiffness showed slight differences. This indicates that it was reasonable and feasible to incorporate the coefficient k into the stiffness calculation equation of RAC beams strengthened with CFRP.

Above all, in the elastic stage of RAC beams strengthened with prestressed CFRP, it is reasonable to introduce coefficient k when calculating stiffness, which can fully show the influence of recycled aggregate content and prestressed CFRP on the stiffness of concrete beams.

The deflection of RAC beams can be obtained using

$$f = \frac{Ml_0^2}{8B_{OA}} \tag{5}$$

where M represents the mid-span bending moment for the beam, $M = PL_0/3$; l_0 is the net span.

3.2.2 Crack Stage

Figs. 10 and 11 show the cross-sectional strain and stress distribution for reinforced RAC beams strengthened by prestressed CFRP under load.

According to the Standard (GB/T 50367-2013, 2013), the stiffness calculation of the RAC beams in this stage is expressed as

$$B_{AB} = \frac{0.85kE_cI_0}{\kappa_{cr} + (1 - \kappa_{cr})\omega} \tag{6}$$

$$\kappa_{cr} = \frac{M_{cr}}{M} \tag{7}$$

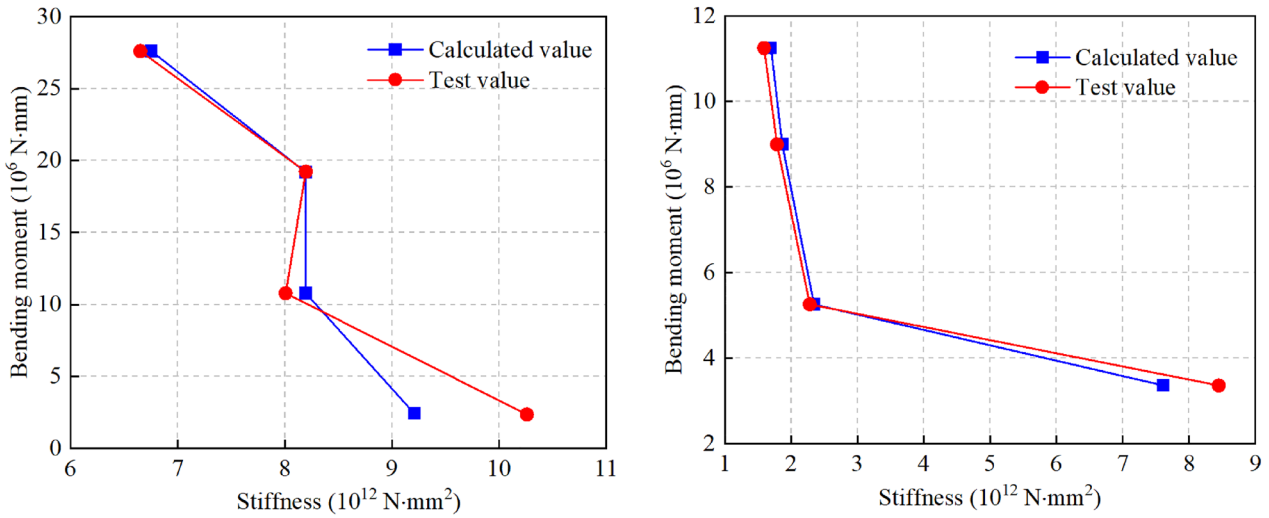


Fig. 9 Comparison between calculated and measured stiffness of reinforced RAC beams strengthened by prestressed CFRP: (left) Xie; (right) Zhao

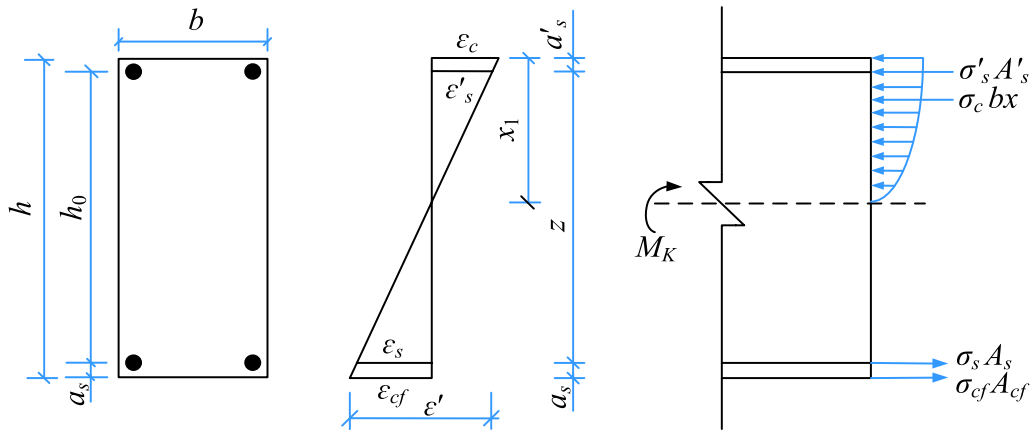


Fig. 10 Cross-sectional strain and stress distribution of reinforced RAC beams strengthened by one layer of prestressed CFRP under loading

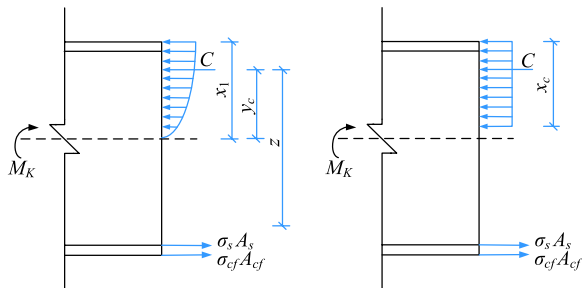


Fig. 11 Equivalent rectangular stress diagram

$$M_{cr} = \frac{\gamma_m f_c I_0}{h - y_0} (0.977 - 0.15833\rho) \tag{8}$$

$$\omega = \left(1 + \frac{0.21}{\alpha_E \rho_{te}}\right) (1 + 0.45\gamma_f) - 0.7 \tag{9}$$

$$\rho_{te} = \frac{A_s + A_{cf-s}}{A_{te}} \tag{10}$$

where κ_{cr} represents the ratio of cracking moment M_{cr} to cracking moment M in the normal section of prestressed concrete flexural members, and when $\kappa_{cr} > 1.0$, κ_{cr} was taken as 1.0; γ_m is the plastic influence coefficient of section resistance moment, which is 1.55; ρ_{te} represents the reinforcement ratio for longitudinal tensile reinforcement; γ_f represents the ratio of the section area of the tensioned flange to the effective section area of the web; A_{te} is the effective tensile concrete section area; A_{cf-s} represents the area of prestressed CFRP and can be obtained

according to the plane section assumption, as shown in Eq. (11).

$$A_{cf-s} = \frac{E_{cf}}{E_s} \times \frac{z + a_s}{z} \times \frac{h_0 - x_1 + a_s}{h_0 - x_1} A_{cf} \quad (11)$$

$$z = y_c + (h_0 - x_1) \quad (12)$$

where z represents the distance from the centroid of the tensile reinforcement to the pressure resultant point of concrete in the compression area; x_1 is the relative height for the compression zone, $x_1 = 3(1-\eta)h_0$, where η is the internal force arm coefficient (about 0.87 (Jiang et al., 2015)); y_c denotes the distance from the resultant force C of reinforcement and concrete in the compression zone to the neutral axis, as shown in Eq. (13).

$$y_c = \frac{\alpha_1 f_c b x_c^2 + \sigma'_s A'_s (h - 2a_{s1})}{2(\alpha_1 f_c b x_c^2 + \sigma'_s A'_s)} \quad (13)$$

where x_c represents the height of the equivalent rectangular compression zone, $x_c = \beta_1 x_1$, where β_1 is the equivalent rectangular stress diagram coefficient and was taken as 0.8.

The deflections are expressed as

$$f_{AB} = f_{g \max} - f_{y \max} \quad (14)$$

$$f_{g \max} = \frac{M l_0^2}{8 B_{AB}} \quad (15)$$

$$f_{y \max} = \frac{N_0 e_0 l_0^2}{8 B_{AB}} \quad (16)$$

where $f_{g \max}$ is the deflection under constant load; $f_{y \max}$ is the camber deflection caused by prestressed CFRP; N_0 is the total tension of the CFRP when the tensile stress is removed, $N_0 = k A_{cf} f_y$; due to the external force, the coefficient k was introduced for reduction, $k = (0.0036P + 0.2694) \times 10^{-3}$, where P is the force; e_0 represents the distance from the neutral axis of the conversion section to the CFRP.

For the beam strengthened by two layers of CFRP, the strain of the second layer was less than that of the first layer when the beam was damaged. Thus, the reinforcement effect of the CFRP was not fully exerted. Therefore, the stress of single layer reinforcement is still considered to solve the beam deflection caused by prestressed CFRP.

3.2.3 Failure Stage

3.2.3.1 Tensile Failure of CFRP The test results show that CFRP was broken when the RAC beam strengthened

with prestressed CFRP was subjected to the ultimate load. The ultimate stiffness of the beam is written as

$$B_{BC} = M/\varphi \quad (17)$$

$$\varphi = \varphi_y + \frac{M - M_y}{M_u - M_y} (\varphi_u - \varphi_y) \quad (18)$$

$$M_y = f_{yk} A_s \left(h_0 - \frac{x_{c-1}}{2} \right) + E_{cf} A_{cf} \varepsilon_{cf} \left(h - \frac{x_{c-1}}{2} \right) \quad (19)$$

$$M_u = \left[f_{stk} A_s \left(h_0 - \frac{x_{c-1}}{2} \right) + E_{cf} A_{cf} (\varepsilon_{cf} + \varepsilon') \left(h - \frac{x_{c-1}}{2} \right) \right] \eta_1 \quad (20)$$

$$\varphi_y = M_y/B_{AB} \quad (21)$$

$$\varphi_u = \frac{\varepsilon'}{h - x} \quad (22)$$

$$x_{c-1} = \frac{\beta_1 \varepsilon_{cu}}{\varepsilon_{cu} + \varepsilon_{cf}} h \quad (23)$$

$$\varepsilon_{cu} = 0.0033 - [f_{cu,k}(1 + \rho) - 50] \times 10^{-5} \quad (24)$$

$$\varepsilon' = \varepsilon_{cf} - \varepsilon'_c \quad (25)$$

$$\varepsilon'_c = \varepsilon_0 \frac{h - x}{x} \quad (26)$$

where φ is the limit curvature; M_y is the yield moment; M_u represents the ultimate bending moment; φ_y is the section curvature at yield; φ_u represents the ultimate curvature corresponding to the ultimate bending moment; f_{yk} represents the yield strength for the steel bar; x_{c-1} represents the height of the compression zone; f_{stk} is the ultimate strength for the steel bar; ε_{cu} represents the ultimate compressive strain of the concrete under non-uniform compression; ε' represents the strain of the concrete at the lower section edge after tensioning; $f_{cu,k}$ represents the compressive strength of the concrete; ε'_c is the leading strain of prestressed CFRP; ε_0 represents the compressive strain when the compressive stress of concrete reaches f_c , which is 0.002.

3.2.3.2 Peeling Failure of CFRP The height of the cross-section compression zone can be expressed as

$$x_{c-2} = \frac{h}{1 + \frac{f_{cf}}{E_{cf} \varepsilon_{cu}} - \frac{\varepsilon_{cf-0}}{\varepsilon_{cu}}} \quad (27)$$

where ϵ_{cf-0} represents the initial effective strain of CFRP, i.e., $4000\mu\epsilon$ in the test; x_{c-2} denotes the height of the compression zone in the rectangular stress diagram. The calculation of rigidity followed Eqs. (17–26) and the calculation of deflection followed Eq. (5).

The stiffness of RAC beams strengthened with pre-stressed CFRP at different stages is expressed as

$$B = \begin{cases} 0.85kE_cI_0 & M < M_{cr} \\ \frac{0.85kE_cI_0}{\kappa_{cr} + (1 - \kappa_{cr})\omega} & M_{cr} < M < M_y \\ M/\varphi & M_y < M < M_u \end{cases} \quad (28)$$

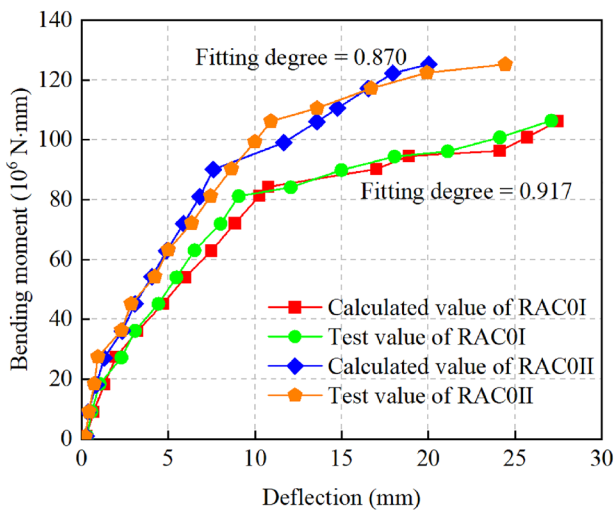
$$f = f_{g \max} - f_{y \max} \quad (29)$$

3.3 Comparison Between Calculated and Measured Deflection

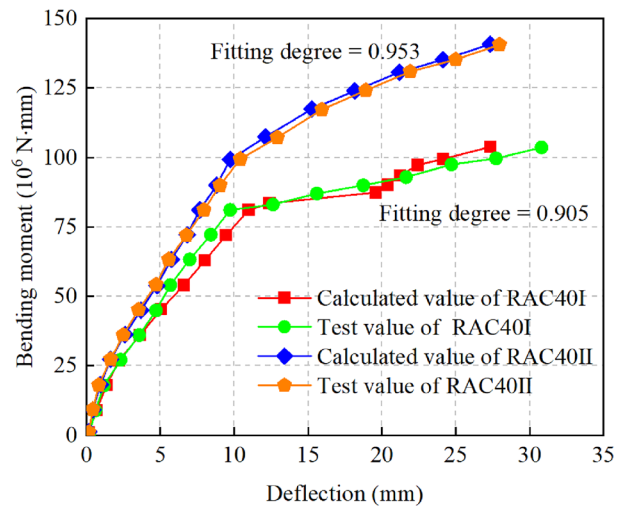
The comparison between the calculated and test beam deflection in Fig. 12 shows that the fitting degree of the two datasets was greater than 0.868. This indicates that the proposed stiffness calculation equation was rational and applicable.

3.4 Analysis of Model Applicability

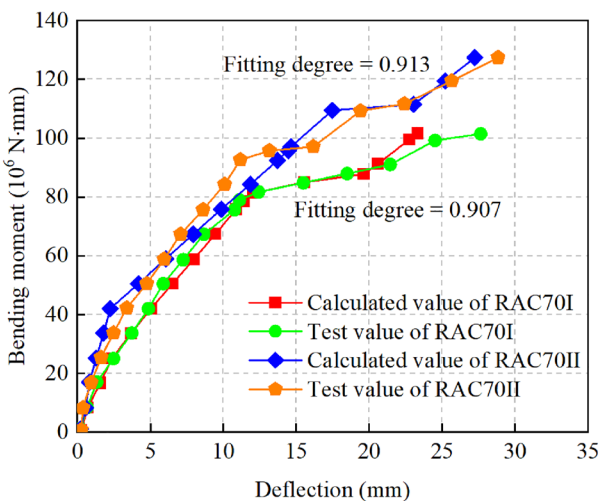
The data from the reference (Gao et al., 2017) were used to prove the applicability of the proposed deflection



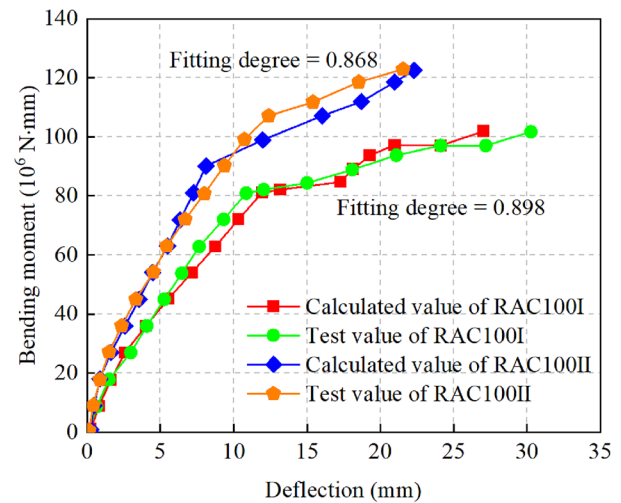
(a)



(b)



(c)



(d)

Fig. 12 Deflection of RAC beams strengthened by CFRP: **a** RAC0; **b** RAC40; **c** RAC70; **d** RAC100

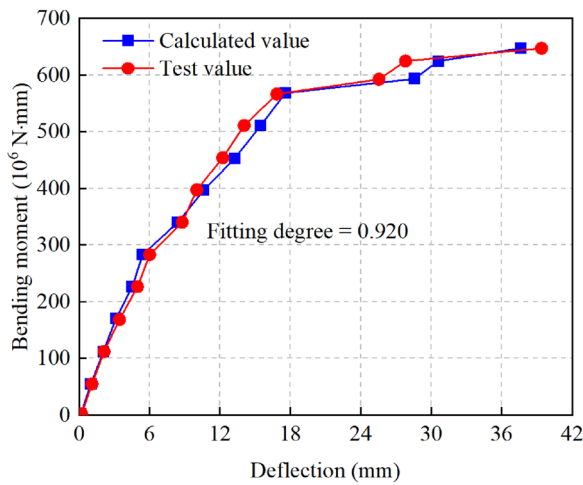


Fig. 13 Bending moment-deflection curves of the mid-span section of the reinforced RAC beams

calculation model. The comparative analysis of the calculated and measured deflection values is displayed in Fig. 13. The average ratio between the calculated and test deflection values is 1.008, with a fit of 0.920. The consistency between the calculated and test deflection indicates that the proposed deflection calculation model can be used to calculate the deflection of RAC strengthened with prestressed CFRP.

4 Calculation of Beam Crack Width

The developed crack width is shown in Table 8. At the same recycled aggregate content, prestressed CFRP of two layers can effectively reduce the beam crack width in the later loading stage. The reason is that prestressed CFRP reduced the stress of steel bars and the strain gradient of the protective layer, and enhanced the bond between tensile material and concrete, thereby reducing the crack width. Under the same CFRP reinforcement layer, an observed trend indicates that the crack width in RAC beams increases proportionally with the increment of recycled aggregate admixture. This phenomenon can be attributed to two primary factors. Firstly, the increase in recycled aggregate admixture results in a reduction in the mechanical properties of the recycled

aggregate. Secondly, the production process of recycled aggregate introduces micro-cracks on its surface. These micro-cracks act as stress concentrators, accelerating the initiation and propagation of cracks within the beams. Consequently, the combined effect of decreased mechanical properties and the presence of micro-cracks contributes to the accelerated generation and expansion of cracks within the RAC beams.

It is the equivalent stress of the steel bar and the non-uniform coefficient of steel bar strain in the tension zone of RAC components that determine the crack width of RAC beams strengthened by prestressed CFRP. According to the Standard (GB/T 50367-2013, 2013), the maximum crack width is calculated using

$$\omega_{\max} = \alpha_{cr} \psi \frac{\sigma_{sq}}{E_s} \left(1.9c_s + 0.08 \frac{d_{eq}}{\rho_{te}} \right) \quad (30)$$

Due to prestressing, Eq. (30) can be converted into Eqs. (31–35) to calculate the crack width:

$$\omega_{\max} = \alpha_{cr} \psi \frac{\sigma_{sk}}{E_s} l_{cr} \quad (31)$$

$$\alpha_{cr} = \alpha_c \tau_s \beta \quad (32)$$

$$\psi = 1.1 - 0.65 \frac{f_{tk}}{\rho_{te} \sigma_{sk}} \quad (33)$$

$$\sigma_{sk} = \varepsilon_s E_s = \frac{M_k - E_{cf} \varepsilon' A_{cf} (z + a_s)}{(A_s + A_{cf-s}) z} \quad (34)$$

$$l_{cr} = \beta \left(1.9c_s + 0.08 \frac{d}{\rho_{te}} \right) \quad (35)$$

where α_{cr} is the characteristic coefficient of the component; τ_s is the nonuniform coefficient of the crack width under the short-term loading. Due to the discrete crack width, the maximum crack width requires an additional expansion coefficient compared with the average crack width. The expansion coefficient was 1.66 for the flexural reinforced concrete beam; α_c is the influence coefficient

Table 8 Comparative analysis of crack width

Bending moment (kN·m)	Crack width (mm)					
	RAC40I	RAC40II	RAC70I	RAC70II	RAC100I	RAC100II
27	0.03	0.02	0.04	0.03	0.08	0.04
36	0.06	0.03	0.06	0.04	0.12	0.05
45	0.09	0.05	0.12	0.06	0.17	0.09
54	0.13	0.08	0.15	0.14	0.21	0.15

of concrete self-elongation between cracks on crack width. With one-layer strengthening, $\alpha_c=0.85$. With two-layer strengthening, $\alpha_c=\varepsilon_{cm}/\varepsilon_{sm}$, where ε_{cm} represents the average tensile strain of side concrete when it is in the same horizontal plane as the longitudinal tensile steel bar; ε_{sm} represents the equivalent average tensile strain of longitudinal steel bars, $\varepsilon_{sm}=\psi\varepsilon_{sk}=\psi\sigma_{sk}/E_s$; ψ is the strain non-uniformity coefficient between cracks of ordinary steel bars under longitudinal tension; σ_{sk} is the equivalent stress for longitudinal steel bars in the tensile zone of prestressed RAC components; l_{cr} is the average crack spacing; d represents the diameter of steel bars; β represents the coefficient related to the stress characteristics for the RAC member: $\beta=1.0$ for flexural, eccentric compression and eccentric tension members, and $\beta=1.1$ for axial tension members.

Table 8 shows that the crack width of RAC beams strengthened with two layers of prestressed CFRP was significantly reduced compared with that of one layer. In addition, the coefficient α_c was related to (e.g.) the reinforcement ratio, the section shape and concrete cover thickness. Since strengthening with two layers of prestressed CFRP reinforcement, α_c cannot be taken as about 0.85, and the influence of various factors should be fully considered.

The crack width was calculated using Eqs. (31–35) and compared with the test results, as displayed in Tables 9 and 10.

The average ratios of calculated to tested values for the crack widths of RAC40I and RAC40II were 1.11 and 1.13 respectively. For RAC70I and RAC70II, the average

ratios were 1.13 and 1.16, respectively. For RAC100I and RAC100II, the average ratios were 1.06 and 1.11, respectively. These results indicate that the crack width calculation model proposed in this paper showed excellent performance.

5 Conclusions

In this paper, calculation models of deflection and crack width of RAC beams strengthened by prestressed CFRP under normal service loads were established. Compared with the test data, the established models showed high accuracy. Thus, this study can provide references for engineering applications.

- (1) The increase in the recycled coarse aggregate content drives down the cracking moment and ultimate load capacity of the beam, while the crack width increases. The increase in the prestressed CFRP strengthening layer reduces the deformation and crack width of the beam, while the number of cracks increases, in addition, it also changes the failure mode of the beam.
- (2) Based on the assumption of plane section and the force balance on the section, a deflection calculation model of the RAC beam strengthened with prestressed CFRP is proposed by using the modified equivalent area of steel bars and the ultimate compressive strain of concrete. Moreover, the fitting degree between the deflection calculated value and the test value of the cited data is as high as 0.92,

Table 9 Crack width of beams strengthened with one layer of CFRP

Bending moment (kN·m)	RAC40I			RAC70I			RAC100I		
	C (mm)	T (mm)	C/T	C (mm)	T (mm)	C/T	C (mm)	T (mm)	C/T
27	0.036	0.03	1.20	0.050	0.04	1.25	0.089	0.08	1.11
36	0.068	0.06	1.13	0.070	0.06	1.17	0.124	0.12	1.03
45	0.100	0.09	1.11	0.122	0.12	1.02	0.175	0.17	1.03
54	0.130	0.13	1.00	0.160	0.15	1.07	0.225	0.21	1.07

C and T represent the calculated and test values, respectively

Table 10 Crack width of beams strengthened with two layers of CFRP

Bending moment (kN·m)	RAC40II			RAC70II			RAC100II		
	C (mm)	T (mm)	C/T	C (mm)	T (mm)	C/T	C (mm)	T (mm)	C/T
27	0.024	0.02	1.20	0.035	0.03	1.17	0.042	0.04	1.05
36	0.033	0.03	1.10	0.043	0.04	1.07	0.053	0.05	1.06
45	0.061	0.05	1.22	0.074	0.06	1.23	0.095	0.09	1.05
54	0.087	0.08	1.01	0.162	0.14	1.16	0.190	0.15	1.27

which indicates that the deflection model established by introducing the coefficient k is reasonable and feasible.

- (3) Considering the influence of prestressed CFRP and RAC, the influence coefficient of concrete elongation on crack width and average crack spacing of beams is revised. A crack width calculation model of RAC beams strengthened with prestressed CFRP is put forward, similar to that for ordinary reinforced concrete beams. The calculated and test values of crack width of RAC beams strengthened with prestressed CFRP are greater than or equal to 1, which proves that the model is accurate.
- (4) The model proposed in this study does not incorporate various influential factors, including temperature fluctuations, shrinkage, RAC creep, and initial loading conditions. As a result, further investigations are necessary to enhance the accuracy and comprehensiveness of this model. By considering these additional parameters, future research endeavors can refine the model and provide a more comprehensive understanding of the behavior and performance of RAC structures. This will ultimately contribute to the advancement of knowledge in the field and enable more reliable predictions and assessments of RAC structural response.

Acknowledgements

The authors would like to acknowledge the editors and reviewers, and their selfless work and valuable comments make a substantial improvement to this manuscript.

Author contributions

YJ and SS performed the experimental works, analyzed data and wrote the manuscript. AC and FY reviewed and commented the manuscript on the crack resistance of RAC beams strengthened with prestressed CFRP. SB and XH reviewed and commented the experimental design, properties of RAC beams strengthened with prestressed CFRP. All authors read and approved the final manuscript.

Funding

This research was supported by the National Natural Science Foundation of China (52179133), the Innovation Funds of NCWU for Doctoral Candidate (B2020081501).

Availability of data and materials

The datasets used and analyzed during the current study are available from the corresponding author on reasonable request.

Declarations

Competing interests

The authors declare that they have no competing interests.

Received: 2 March 2023 Accepted: 26 August 2023
Published online: 04 January 2024

References

- Bakar, M. B. C., Muhammad, R. S. M., Amran, M., Jaafar, M. S., Vatin, N. I., & Fediuk, R. (2022). Flexural strength of concrete beam reinforced with CFRP bars: A review. *Materials*. <https://doi.org/10.3390/ma15031144>
- Chen, A.J., Zhao, S.B., Li, C.Y., & Wang, J. (2013). Construction method for strengthening concrete beam with prestressed carbon fiber reinforced plastics.
- Chen, B. F. (2013). Basic mechanical properties and microstructural analysis of recycled concrete. *Journal of Wuhan University of Technology-Mater. Sci. Ed.*, 28(1), 104–109. <https://doi.org/10.1007/s11595-013-0649-x>
- Chen, G. M., He, Y. H., Jiang, T., & Lin, C. J. (2016). Behavior of CFRP-confined recycled aggregate concrete under axial compression. *Construction and Building Materials*, 111, 85–97. <https://doi.org/10.1016/j.conbuildmat.2016.01.054>
- Colalillo, M. A., & Sheikh, S. A. (2012). Seismic retrofit of shear-critical reinforced concrete beams using CFRP. *Construction and Building Materials*, 32, 99–109. <https://doi.org/10.1016/j.conbuildmat.2010.12.065>
- Dimitriou, G., Savva, P., & Petrou, M. F. (2018). Enhancing mechanical and durability properties of recycled aggregate concrete. *Construction and Building Materials*, 158, 228–235. <https://doi.org/10.1016/j.conbuildmat.2017.09.137>
- Eljufout, T., Toutanji, H., & Al-Qaralleh, M. (2021). Effect of CFRP strengthening systems on the fatigue limit of reinforced concrete beams. *Structure and Infrastructure Engineering*, 17(3), 361–378. <https://doi.org/10.1080/15732479.2020.1751665>
- ElSafty, A., Graeff, M. K., & Fallaha, S. (2014). Behavior of laterally damaged prestressed concrete bridge girders repaired with CFRP laminates under static and fatigue loading. *International Journal of Concrete Structures and Materials*, 8(1), 43–59. <https://doi.org/10.1007/s40069-013-0053-0>
- Gao, D. Y., Wang, T. Y., & He, Y. J. (2017). Flexural test and calculation on capacity of reinforced concrete short beam strengthened by CFRP sheets. *Journal of Building Structures*, 38(11), 122–131. <https://doi.org/10.14006/jjzjgxb.2017.11.014>
- Gao, P., Gu, X. L., & Mosallam, A. S. (2016). Flexural behavior of preloaded reinforced concrete beams strengthened by prestressed CFRP laminates. *Composite Structures*, 157, 33–50. <https://doi.org/10.1016/j.compstruct.2016.08.013>
- GB/T 25177-2010. (2010). Recycled coarse aggregate for concrete. Beijing, China.
- GB/T 50010-2010. (2010). Code for design of concrete structures. Beijing, China.
- GB/T 50081-2019. (2019). Standard for test methods of concrete physical and mechanical properties. Beijing, China.
- GB/T 50367-2013. (2013). Code for design of strengthening concrete structure. Beijing, China.
- Han, F. (2019). *Flexural behavior of steel fiber-reinforced recycled aggregate concrete beams with BFRP rebars*. Liaoning University of Technology.
- Helal, K., Yehia, S., Hawileh, R., & Abdalla, J. (2020). Performance of preloaded CFRP-strengthened fiber reinforced concrete beams. *Composite Structures*, 244, 112262. <https://doi.org/10.1016/j.compstruct.2020.112262>
- Huang, H., Wang, W. W., Dai, J. G., & Brigham, J. C. (2017). Fatigue behavior of reinforced concrete beams strengthened with externally bonded prestressed CFRP sheets. *Journal of Composites for Construction*. [https://doi.org/10.1061/\(ASCE\)CC.1943-5614.0000766](https://doi.org/10.1061/(ASCE)CC.1943-5614.0000766)
- Huang, J., Shi, J., Xiao, H. H., Shen, J. Y., & Yang, B. S. (2020). Stressing state analysis of reinforcement concrete beams strengthened with carbon fiber reinforced plastic. *International Journal of Concrete Structures and Materials*, 14(5), 745–766. <https://doi.org/10.1186/s40069-020-00417-w>
- JGJ 55-2011. (2011). Specification for mix proportion design of ordinary concrete. Beijing, China.
- Jiang, S. H., Hou, J. G., & He, Y. M. (2015). Reliability research of serviceability limit states for RC beams strengthened with prestressed CFRP sheets considering prestress loss. *China Civil Engineering Journal*, 48(11), 8. <https://doi.org/10.15951/j.tmgcxb.2015.11.006>
- Kadhim, M. M. A., Altaee, M. J., Adheem, A. H., Chabuk, A., & Al-Ansari, N. (2021). Review on NSM CFRP strengthened RC concrete beams in shear.

Advances in Civil Engineering., 2021, 1–16. <https://doi.org/10.1155/2021/1074010>

- Khan, A., Fareed, S., Nasir, R., & Xiao, J. Z. (2021). Behaviour and strength prediction of reinforced recycled aggregate concrete columns confined with CFRP wraps. *Iranian Journal of Science and Technology, Transactions of Civil Engineering.*, 46(4), 2777–2789. <https://doi.org/10.1007/s40996-021-00779-5>
- Liu, Y., Peng, H., & Cai, C. S. (2015). A probabilistic model for the flexural capacity of reinforced concrete structures strengthened with prestressed CFRP plates. *Advances in Structural Engineering.*, 18(5), 629–642. <https://doi.org/10.1260/1369-4332.18.5.629>
- Lotfy, A., & Al-Fayez, M. (2015). Performance evaluation of structural concrete using controlled quality. *Cement and Concrete Composites.*, 61, 36–43. <https://doi.org/10.1016/j.cemconcomp.2015.02.009>
- Medina, C., Zhu, W.Z., Howind, T., deRojas, M.I.S., & Frias, M. (2014). Influence of mixed recycled aggregate on the physical–mechanical properties of recycled concrete. *J. Clean Prod.*, 68, 216–225. <https://doi.org/10.1016/j.jclepro.2014.01.002>
- McNeil, K., & Kang, T. (2013). Recycled concrete aggregates a review. *International Journal of Concrete Structures and Materials.*, 7(1), 61–69. <https://doi.org/10.1007/s40069-013-0032-5>
- Ozbakkaloglu, T., Gholampour, A., & Xie, T. Y. (2018). Mechanical and durability properties of recycled aggregate concrete: Effect of recycled aggregate properties and content. *Journal of Materials in Civil Engineering.* [https://doi.org/10.1061/\(ASCE\)MT.1943-5533.0002142](https://doi.org/10.1061/(ASCE)MT.1943-5533.0002142)
- Shakirov, A., Sulejmanov, A. (2021). Prediction of creep for a reinforced concrete beam strengthened with an external reinforcement system using the stepped isothermal method, international scientific conference on socio-technical construction and civil engineering. Springer
- Song, L., & Hou, J. (2017). Fatigue assessment model of corroded RC beams strengthened with prestressed CFRP sheets. *International Journal of Concrete Structures and Materials.*, 11(2), 247–259. <https://doi.org/10.1007/s40069-017-0191-x>
- Tan, Y. S. (2019). *Research on uniaxial compression constitutive relationship and damage model of recycled concrete.* Beijing University of Civil Engineering and Architecture.
- Toledo, R. D., Koenders, E., Pepe, M., Cordeiro, G. C., Fairbairn, E., & Martinelli, E. (2013). Rio 2016 sustainable construction commitments lead to new developments in recycled aggregate concrete. *Proceedings of the Institution of Civil Engineers-Civil Engineering.*, 166(6), 28–35. <https://doi.org/10.1680/cien.13.00010>
- Wang, B., Yan, L. B., Fu, Q. N., & Kasal, B. (2021). A comprehensive review on recycled aggregate and recycled aggregate concrete. *Resources, Conservation and Recycling.*, 171, 105565. <https://doi.org/10.1016/j.resconrec.2021.105565>
- Xie, B. (2019). *Experimental study on flexural behavior of concrete beams strengthened with prestressed CFRP tendons.* Guangxi University of Science and Technology.
- Xie, T. Y., Gholampour, A., & Ozbakkaloglu, T. (2018). Toward the development of sustainable concretes with recycled concrete aggregates: Comprehensive review of studies on mechanical properties. *Journal of Materials in Civil Engineering.* [https://doi.org/10.1061/\(ASCE\)MT.1943-5533.0002304](https://doi.org/10.1061/(ASCE)MT.1943-5533.0002304)
- Xue, W. C., Tan, Y., & Zeng, L. (2010). Flexural response predictions of reinforced concrete beams strengthened with prestressed CFRP plates. *Composite Structures.*, 92(3), 612–622. <https://doi.org/10.1016/j.compstruct.2009.09.036>
- Yehia, S., Helal, K., Abusharkh, A., Abusharkh, A., Zaher, A., & Istaitiyeh, H. (2015). Strength and durability evaluation of recycled aggregate concrete. *International Journal of Concrete Structures and Materials.*, 9(2), 219–239. <https://doi.org/10.1007/s40069-015-0100-0>
- Zhang, L. W., Sojobi, A. O., & Liew, K. M. (2019). Sustainable CFRP-reinforced recycled concrete for cleaner eco-friendly construction. *Journal of Cleaner Production.*, 233, 56–75. <https://doi.org/10.1016/j.jclepro.2019.06.025>
- Zhao, L. J., Dou, T. S., Cheng, B. Q., Xia, S. F., Yang, J. X., Zhang, Q., Li, M., & Li, X. L. (2019). Theoretical study and application of the reinforcement of prestressed concrete cylinder pipes with external prestressed steel strands. *Applied Sciences.*, 9(24), 5532. <https://doi.org/10.3390/app9245532>
- Zhao, M. Q. (2017). *Research on mechanical properties of reinforced concrete beams reinforced with CFRP.* Anhui Jianzhu University.

Publisher's Note

Springer Nature remains neutral with regard to jurisdictional claims in published maps and institutional affiliations.

Yanting Ji Ph.D. School of Water Conservancy

Sheng Sun M.Eng., School of Civil Engineering and Communication

Aijiu Chen Ph.D. Professor, Doctoral advisor, School of Civil Engineering and Communication

Fen Yang Master, Staff, Zhengzhou Zoo

Shihua Bai Master, Staff, Henan Zhongyu Engineering Consulting Group Co., Ltd.

Xiaoyan Han Ph.D. Lecturer, School of Civil Engineering and Communication

Submit your manuscript to a SpringerOpen[®] journal and benefit from:

- Convenient online submission
- Rigorous peer review
- Open access: articles freely available online
- High visibility within the field
- Retaining the copyright to your article

Submit your next manuscript at ► [springeropen.com](https://www.springeropen.com)